

MECHANICS OF CARBON NANOSCROLLS: A REVIEW

Xinghua Shi¹ Nicola M. Pugno² Huajian Gao^{1*}

(¹*School of Engineering, Brown University, 610 Barus & Holley, 182 Hope Street, Providence, RI 02912, USA*)

(²*Laboratory of Bio-inspired Nanomechanics 'Giuseppe Maria Pugno', Department of Structural Engineering, Politecnico di Torino, Corso Duca degli Abruzzi 24, 10129, Torino, Italy*)

Received 16 September 2010; revision received 23 November 2010

ABSTRACT Carbon nanoscrolls (CNSs) belong to the same class of carbon-based nanomaterials as carbon nanotubes but are much less studied in spite of their great potential for applications in nanotechnology and bioengineering. Fundamental description, understanding and regulation of such materials will ultimately lead to a new generation of integrated systems that utilize their unique properties. In this review, we describe some of the recent advances in theoretical investigation on structural and dynamical behavior of CNS, as well as relevant simulation techniques. Theoretically it has been found that a stable equilibrium core size of CNS can be uniquely determined or tuned from the basal graphene length, the interlayer spacing, the interaction energy between layers of CNS and the bending stiffness of graphene. Perturbations of the surface energy, which can be controlled by an electric field, will cause a CNS to undergo breathing oscillatory motion as well as translational rolling motion on a substrate. The tunable core size of CNS also enables it to serve potentially as transmembrane water channels in biological systems.

I. INTRODUCTION

Carbon nanoscrolls (CNSs) have attracted significant interests in recent years^[1–6]. Unlike the tubular structure of carbon nanotubes (CNT), a CNS is made of a continuous graphene sheet rolled up in a spiral form. CNS was first discovered in a chemical synthesis route when graphite was intercalated with potassium metal, exfoliated with ethanol and then sonicated^[1]. Recently, a simple and effective way has been developed to fabricate CNS on SiO₂/Si substrate, in which a graphene sheet extracted mechanically from graphite was found to spontaneously roll into CNS in isopropyl alcohol (IPA) solvent^[2]. Due to their unique topology, CNSs have shown unique structural^[7–11], dynamical^[8] and electronic^[2, 7, 12, 13] properties. More specifically, a stable formation of CNS was found to exist with energy lower than that of the precursor graphene^[8]. The core of CNS can be significantly changed upon charge injection, which makes it a natural choice for a new class of efficient nanoactuators^[13]. The flexible core and large surface area also enable the CNS to be potential utilized for hydrogen storage^[9–11]. Recent experiments on electrical-transport measurements^[2] show that the resistance of CNS is weakly gate-dependent but strongly temperature-dependent. In addition, the CNS can sustain a high current density, suggesting that it might be a good candidate for microcircuit interconnects.

Among various potential interests, the mechanics of CNS is an important issue that must be addressed in order to apply CNS successfully in future devices. Of particular interest is the fundamental basis for stability^[14, 15], structural and dynamical behaviors of CNS^[16–19]. The present paper is aimed at a review of recent theoretical studies as well as molecular dynamics (MD) simulations of the mechanical properties and behaviors of CNSs.

* Corresponding author. E-mail: huajian_gao@brown.edu

II. EQUILIBRIUM CORE SIZE OF CARBON NANOSCROLLS

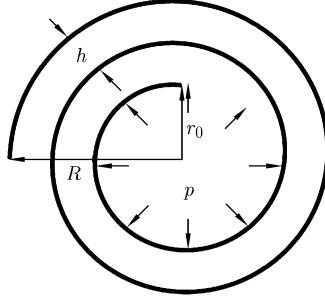


Fig. 1. Schematic illustration of a carbon nanoscroll with inner radius r_0 , outer radius R and interlayer spacing h , subjected to pressure p .

The equilibrium core size of CNS has been obtained theoretically and verified by MD simulations^[14,15]. Consider a free standing CNS rolled up from a graphene sheet of length B and width L , with inter core radius r_0 , outer radius R and interlayer spacing h (Fig.1). The total free energy of this system is composed of three terms: the elastic bending energy, the surface energy and the work done by the pressure. Under an infinitesimal variation in core radius r_0 , the change in bending energy of the scroll is

$$dW = -\frac{\pi DL}{h} \frac{R^2 - r_0^2}{R^2} \frac{dr_0}{r_0} \quad (1)$$

where D is the bending stiffness. On the other hand, the change in total surface energy of the CNS is

$$d\Gamma = 2\pi\gamma L (dr_0 + dR) = 2\pi\gamma L \left(1 + \frac{r_0}{R}\right) dr_0 \quad (2)$$

where γ is the surface energy per unit area. The corresponding work done by the pressure is

$$d\Phi = -p_i 2\pi L r_0 dr_0 + p_e 2\pi L R dR = -2\pi L r_0 dr_0 p \quad (3)$$

where $p = p_i - p_e$, p_e and p_i being the external and internal pressures of CNS, respectively. The equilibrium core size can be calculated by setting $dE = dW + d\Gamma + d\Phi = 0$, which yields

$$\frac{2\gamma h}{D} = \frac{1}{r_0} - \frac{1}{R} + \frac{2hp}{D(1/r_0 + 1/R)} \quad (4)$$

or

$$p(r_0) = \frac{D}{2h} \left(\frac{2\gamma h}{D} - \frac{1}{r_0} + \frac{1}{R} \right) \left(\frac{1}{r_0} + \frac{1}{R} \right) \quad (5)$$

where $R = \sqrt{Bh/\pi + r_0^2}$.

The stability of the system requires $d^2E/dr^2 \geq 0$. Under constant pressure, this condition is reduced to

$$\frac{d^2E}{dr_0^2} = \frac{DBL}{R^2 r_0^2} + \frac{2DBL}{R^4} + 2\pi\gamma L \left(\frac{1}{R} - \frac{r_0^2}{R^3} \right) - 2\pi L (p_i - p_e) \geq 0 \quad (6)$$

Taking the parameters as $D=0.11$ nN·nm, $\gamma = 0.4$ nN/nm, $h=0.34$ nm and $B=200$ nm, Fig.2 shows the second derivative of the free energy with respect to the core size. In the absence of a pressure difference ($p = p_i - p_e = 0$), d^2E/dr^2 is always greater than zero, indicating that the equilibrium configuration of CNS is stable. Figure 3(a) shows how the surface energy, the bending stiffness, the interlayer spacing of graphene and the length of graphene sheet influence the core size of the CNS. Figure 3(b) plots evolution of the potential energy (elastic energy plus surface energy) as a function of the core size. The results shown in Figs.2 and 3 clearly indicate that there exists a stable configuration of CNS with

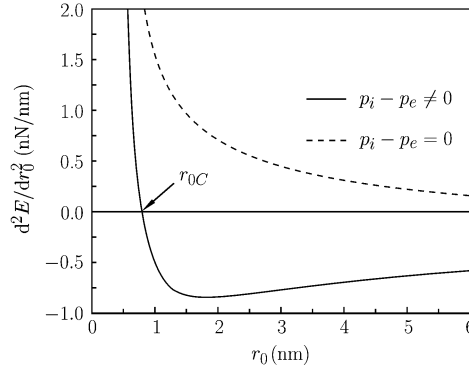


Fig. 2. Second derivative of the free energy of a CNS with respect to its core size. The dashed line is for the case without pressure difference ($p_i - p_e = 0$) and solid line for a finite pressure difference ($p_i - p_e \neq 0$)^[15].

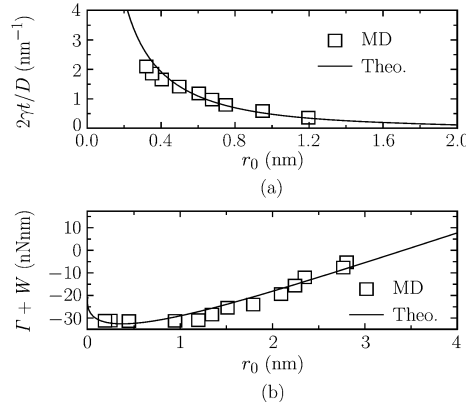


Fig. 3. (a) The ratio between surface energy and bending modulus of graphene as a function of the CNS core size, (b) the potential energy as a function of the core size. All results are obtained in vacuum. The squares are the MD results and solid line is the theoretical prediction^[14].

an equilibrium core size. Under constant pressure $p = p_i - p_e \neq 0$, however, d^2E/dr^2 is greater than zero only when the core size is below some critical value r_{0C} (Fig.2). This indicates that there is a critical pressure for a given core radius or a critical core size for a given pressure, beyond which the CNS becomes mechanically unstable.

MD simulations have been performed to verify the theoretical predictions. In particular, the package Gromacs 4 has been used to simulate the core size of CNS^[20]. The graphene is described by a Morse bond, a harmonic cosine term for the bond angle, a cosine term for torsion and a Lennard-Jones (L-J) term for the van der Waals (vdW) interaction as^[21]

$$U(r_{ij}, \theta_{ijk}, \phi_{ijkl}) = K_{Cr} \left[e^{-k_C(r_{ij} - r_C)} - 1 \right]^2 + \frac{1}{2} K_{C\theta} (\cos \theta_{ijk} - \cos \theta_C)^2 + \frac{1}{2} K_{C\phi} [1 - \cos(2\phi_{ijkl})] + 4\varepsilon_{CC} \left[\left(\frac{\sigma_{CC}}{r_{ij}} \right)^{12} - \left(\frac{\sigma_{CC}}{r_{ij}} \right)^6 \right] \quad (7)$$

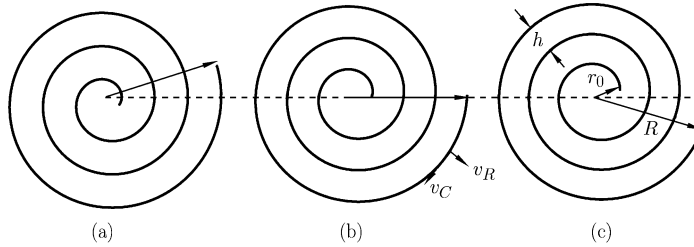
where k_C defines the steepness of the Morse potential well, r_{ij} denotes the distance between two bonded atoms, θ_{ijk} and ϕ_{ijkl} are the bending and torsional angles, r_C, θ_C and ϕ_C are the reference geometrical parameters for graphene, $K_{Cr}, K_{C\theta}$ and $K_{C\phi}$ are the force constants of stretching, bending and torsion, respectively, whereas σ_{CC} and ε_{CC} are the L-J parameters for carbon. Selected values of the simulation parameters are listed in Table 1. Room temperature (300 K) and atmospheric pressure (1 bar) are maintained in all simulations. The MD results agree well with the theoretical predictions (Fig.3), indicating that the theoretical model is capable of predicting the core size of CNS.

Table 1. Parameters of interaction potential used in the molecular dynamics simulations^[21]

$K_{Cr} = 47890 \text{ kJmol}^{-1}\text{nm}^{-2}$	$r_C = 0.142 \text{ nm}$	$k_C = 21.867 \text{ nm}^{-1}$
$K_{C\theta} = 562.2 \text{ kJmol}^{-1}$	$\theta_C = 120^\circ$	$\varepsilon_{CC} = 0.4396 \text{ kJmol}^{-1}$
$K_{C\phi} = 25.12 \text{ kJmol}^{-1}$	$\phi_C = 180^\circ$	$\sigma_{CC} = 0.385 \text{ nm}$

III. BREATHING MOTION OF CNS

One possible application of CNS is a nano-oscillator with high breathing oscillatory frequency. The breathing motion of CNS has been investigated via theoretical model and MD simulations^[16]. Figure 4 illustrates schematically the breathing oscillatory motion of a CNS. Such oscillation can be initiated by suddenly decreasing the interlayer interaction energy to generate a small perturbation in the system. As a consequence of this perturbation, the CNS starts to oscillate with periodic expansion and contraction phases with circumferential velocity v_C and radial velocity v_R . During the expansion phase, the kinetic energy first increases as the potential energy decreases to a minimum value (Fig.4(b)) and then decreases as the potential energy increases to a maximum value (Fig.4(c)). At that point, the contraction phase starts, with potential and kinetic energies going through a similar cycle of growth and decay as in the expansion phase. In this way, the CNS moves back to its initial configuration (Fig.4(a)) and one oscillatory cycle is completed.

Fig. 4. The breathing oscillatory motion of a carbon nanoscroll^[16].

To quantify the above oscillatory motion, it will be convenient to consider the core radius of a CNS as the controlling degree of freedom. It has been previously shown that a stable equilibrium value of r_0 can be uniquely determined from the basal graphene length B , the interlayer spacing h , the interaction energy γ and the bending stiffness D . Given the existence of such an equilibrium value for r_0 , the breathing oscillation is defined as the oscillatory motion associated with slight perturbations of r_0 from its equilibrium value. The breathing motion of the CNS can be described using Lagrange's equation

$$\frac{\partial (K - V)}{\partial r_0} - \frac{d}{dt} \frac{\partial (K - V)}{\partial \dot{r}_0} - \frac{\partial F}{\partial \dot{r}_0} = 0 \quad (8)$$

where K denotes the kinetic energy and V the potential energy; F is Rayleigh's dissipation function, t is the time and over-dot represents time derivative. The potential energy of the system is obtained as

$$V = \frac{\pi DL}{h} \ln \left(\frac{R}{r_0} \right) + 2\pi\gamma L (r_0 + R) - \pi r_0^2 L p \quad (9)$$

The kinetic energy in the system could be evaluated as

$$K = \frac{1}{2} M v_C^2 = \frac{2\pi^2 M r_0^2 \dot{r}_0^2}{h^2} \quad (10)$$

where M is the total mass of the CNS. There also exists a viscous damping force with $\partial F / \partial \dot{r}_0 = C(T) \dot{r}_0$, where $C(T)$ is a damping coefficient which depends on the temperature T of the system. Combining all terms together, the Lagrange equation of motion is derived as

$$\begin{aligned} \frac{\pi DL}{h} \left(1 - \frac{r_0^2}{Bh/\pi + r_0^2} \right) \frac{1}{r_0} - 2\pi\gamma L \left(1 + \frac{r_0}{\sqrt{Bh/\pi + r_0^2}} \right) \\ + 2\pi r_0 L p - \frac{4\pi^2 M}{h^2} (r_0 \dot{r}_0^2 + r_0^2 \ddot{r}_0) - C \dot{r}_0 = 0 \end{aligned} \quad (11)$$

which can be used to study dynamic expansion/contraction of a CNS. In particular, for the breathing oscillatory motion around an equilibrium configuration, a solution in the form $r_0(t) = r_{0e} + \varepsilon(t)$ needs to be solved, where $\varepsilon(t)$ is a small perturbation and r_{0e} is a static equilibrium core size satisfying Eq.(4). For small perturbations $\varepsilon(t)$, only first order terms $\varepsilon, \dot{\varepsilon}, \ddot{\varepsilon}$ are kept in the Lagrange equation and a governing equation for the breathing oscillation as $\ddot{\varepsilon} + 2\zeta\omega_0\dot{\varepsilon} + \omega_0^2\varepsilon = 0$ is obtained, where

$$\omega_0 = \sqrt{\frac{\pi D}{4\rho B^3 h^2} \left[\frac{\alpha^3(\alpha+3)}{(1+\alpha)^2} + 2\frac{\gamma}{D} \sqrt{\frac{Bh^3}{\pi}} \frac{\alpha^2\sqrt{\alpha}}{(1+\alpha)^{3/2}} - 2\frac{Bh^2 p}{\pi D} \alpha \right]} \quad (12)$$

is identified as the oscillation frequency and

$$\zeta = \frac{C\alpha}{8\pi\rho LB^2\omega_0} \quad (13)$$

is the effective damping factor. Here, ρ is the material density and $\alpha = Bh/(\pi r_{0e}^2)$ is the ratio between the cross-sectional area of the CNS and that inside the core. Equation (12) suggests that the oscillatory frequency ω_0 is related to the bending modulus D , the surface energy γ , the length of graphene B , the interlayer spacing h and the relative pressure p . The effective damping ζ is related to the frequency ω_0 , the CNS width L as well as the damping coefficient C .

Figure 5(c) plots the relation between the oscillatory frequency and surface energy by taking the rest of the parameters as $p=0$, $B=24$ nm, $D=0.11$ nNnm, $\rho = 2267$ kg/m³ and $h=0.34$ nm. The result indicates that the oscillatory frequency increases with the surface energy. On the other hand, if the surface energy is fixed at $\gamma = 0.1$ nN/nm, Fig.5(d) shows the oscillatory frequency as a function of the graphene length B , indicating that the frequency can be raised by shortening the graphene length.

To verify the theoretical model, MD simulations are conducted with the non-bonded vdW interactions as described by the L-J potential

$$U(r_{ij}, \lambda) = 4\lambda\varepsilon_{CC} \left[\left(\frac{\sigma_{CC}}{r_{ij}} \right)^{12} - \left(\frac{\sigma_{CC}}{r_{ij}} \right)^6 \right] \quad (14)$$

where $\varepsilon_{CC} = 0.3601$ kJ/mol, $\sigma_{CC} = 0.34$ nm and λ is a tuning parameter ($0 < \lambda \leq 1$) that can be used to tune the core size of a CNS. In MD simulations of oscillation around an equilibrium configuration characterized by a specific λ , an initial equilibrium structure is set up at a slightly perturbed state $\lambda + \delta\lambda$, where $\delta\lambda$ is typically taken to be 0.2. The oscillation of the CNS is initiated by setting the tuning parameter back to the reference value λ . Experimentally, the small perturbation $\delta\lambda$ can be imposed by applying an electric field to reduce the effective surface energy of the CNS^[18]. The simulations are conducted using LAMMPS^[22] with microcanonical NVE ensemble, initial temperature 10 K and time step 1 fs.

The simulation results confirm the gigahertz breathing oscillatory motion of CNSs (Figs.5(a) and 5(c)). The theoretical result in Eq.(12) shows that the oscillating frequency depends on the surface energy which is controlled by the vdW interaction parameter λ in the simulations. The results of an armchair CNS with the same length $B = 24$ nm show similar behaviors as that of the zigzag CNS (Figs.5(b) and 5(c)), suggesting that the effect of chirality on the oscillating frequency is relatively minor. It is found that the shorter the graphene length, the higher the oscillating frequency (Figs.5(d)). Figs.5(c) and 5(d) show that the MD results are in good agreement with the corresponding predictions from our theoretical model.

An interesting question is how a CNS responds to an applied oscillating field near the resonant frequency of the system. To mimic an applied AC electric field, the energy tuning parameter varies according to

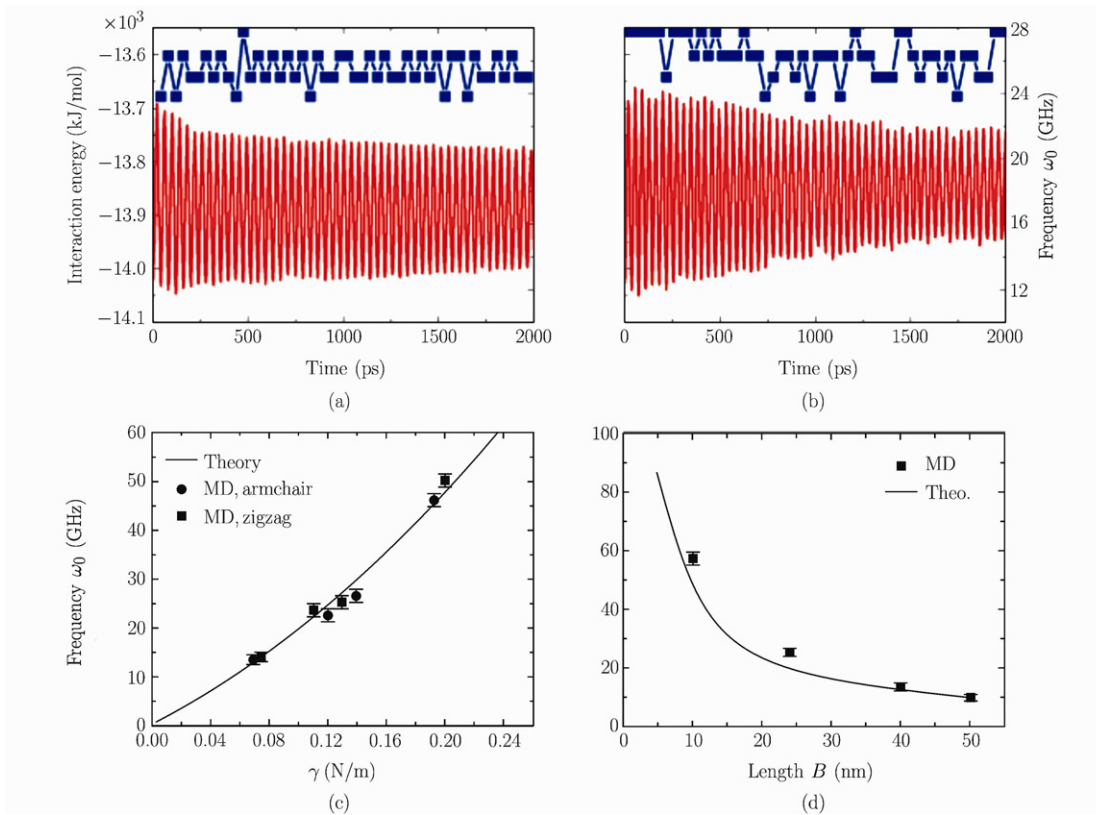


Fig. 5. Gigahertz oscillatory motion of carbon nanoscrolls (CNSs). MD simulation results for the interlayer interaction energy (red line) and fundamental frequency (blue square) as functions of time for (a) zigzag or (b) armchair CNSs. The length B of the basal graphene sheet is taken to be 24 nm and tuning parameter λ is 0.8, (c) the fundamental frequency as a function of the surface energy of CNSs. The solid line is the theoretical prediction, whereas the squares or circles are the simulation results for zigzag or armchair CNSs, respectively, (d) the fundamental frequency as a function of the graphene length. The solid line is the theoretical prediction, and the squares are the simulation results for zigzag CNSs^[16].

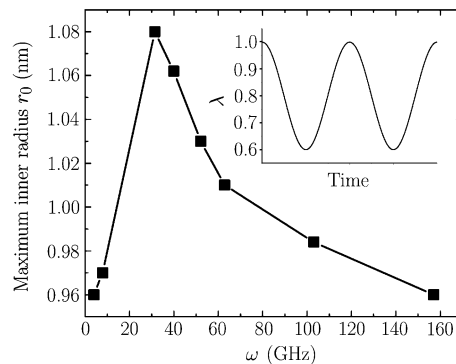


Fig. 6. The maximum core radius of a CNS subjected to an oscillating interlayer interaction energy with frequency ω (inset), simulating resonance under an applied AC electric field^[16].

$$\lambda(t) = \frac{1 - \beta}{2} [1 + \cos(\omega t)] + \beta \quad (15)$$

where ω is the frequency of the applied field and β is a parameter depending on the field strength. Consider a simulation system with $B = 24$ nm and $\beta = 0.6$, λ varies from 0.6 to 1 with a mean value of 0.8 (see the inset of Fig.6). Figure 6 shows that the maximum inner core radius varies with the applied frequency ω , with a peak value at $\omega \sim 30$ GHz, which is quite close to the fundamental frequency about 27 GHz at $\lambda = 0.8$ for the selected CNS. Note that the core of the CNS is significantly widened at the

resonant frequency. This phenomenon may be particularly useful in designing controllable CNS-based drug and gene loading/release systems.

IV. ROLLING MOTION OF CNS ON SUBSTRATE

The previous studies have been focused on the behaviors of a free standing CNS. Inspired by recent experiments on the fabrication of CNSs on solid substrates^[2], the authors have developed a theory of linear actuator based on substrate-supported CNSs; they conduct molecular dynamics simulations to demonstrate the principle of such linear actuation through controlled forward and backward rolling of a CNS on a graphite substrate as its surface energy is tuned by an applied DC/AC electric field^[17].

Figure 7 displays some snapshots from MD simulations of a linear nanoactuator based on a CNS supported on a graphite substrate. A multiwalled carbon nanotube (MWCNT) has been added to the system to aid the initial formation of the CNS^[19] as well as to constrain its inner core size during linear motion. With fixed CNS-substrate interaction, the CNS would roll rightward if the CNS-CNS interaction is strong enough to overcome the CNS-graphite interaction as well as the contribution from elastic bending of CNS (Fig.7(a)). On the other hand, it would roll leftward if the CNS-CNS interaction is reduced by an applied electric field (Fig.7(b)). In this manner, the CNS is controlled to move rightward or leftward by tuning the CNS-CNS interaction energy.

Consider a CNS rolled up from a graphene sheet of length B and width L on a rigid substrate (Fig.8). The nanoscroll has a fixed inner core radius r_0 , outer radius R and interlayer spacing h , and can be rolled out into a flat graphene sheet along the substrate. In this process, the nanoscroll part of the structure can be described by a radial function as $r = r_0 + [h/(2\pi)]\vartheta$, where B , h , R and r_0 are related as $\pi(R^2 - r_0^2) = (B - x)h$, where x denotes the length of the rolled out part of the graphene sheet on substrate. As the CNS is unrolled by an infinitesimal distance δx , the outer radius R of the CNS would decrease by $2\pi R\delta R = -h\delta x$. The change in strain energy is then

$$\delta W = \frac{\pi DL}{h} \frac{\delta R}{R} = -\frac{DL}{2[(B-x)h/\pi + r_0^2]} \delta x \quad (16)$$

At the same time, the total surface energy of the CNS is altered by

$$\delta \Gamma = L(\gamma_{CC} - \gamma_{CS}) \delta x \quad (17)$$

where γ_{CC} is the interlayer interaction energy of CNS and γ_{CS} is the interaction energy per unit area between the rolled out graphene sheet and substrate. Adding the contributions from elastic energy and surface energy, the change in total potential energy associated with an unrolling displacement δx is

$$\frac{\delta V}{\delta x} = \frac{\delta \Gamma}{\delta x} + \frac{\delta W}{\delta x} \quad (18)$$

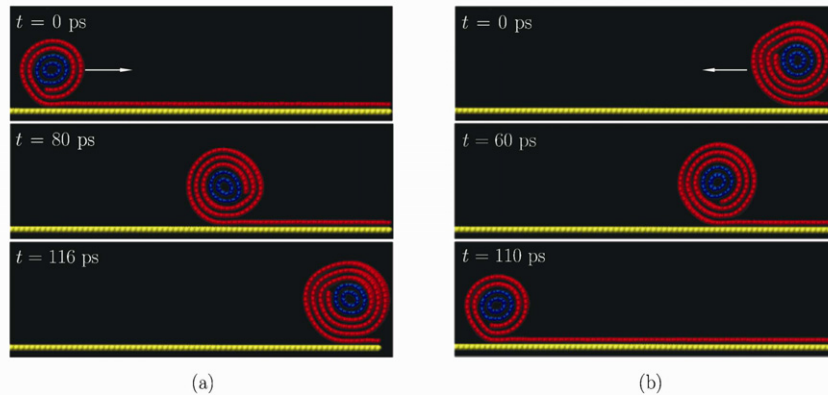


Fig. 7. Snapshots of molecular dynamics simulation of carbon nanoscrolls (CNS) (red color) rolling along the graphite substrate (yellow color). The tuning parameter for CNS-CNS interaction is (a) $\lambda_{CC} = 1.0$ or (b) $\lambda_{CC} = 0.6$. The tuning parameter for CNS-Graphite interaction is $\lambda_{CS} = 0.8$ in both systems. To constrain the core size of CNS, a multi-walled carbon nanotubes (MWCNT) is inserted inside the core of CNS (blue color)^[17].

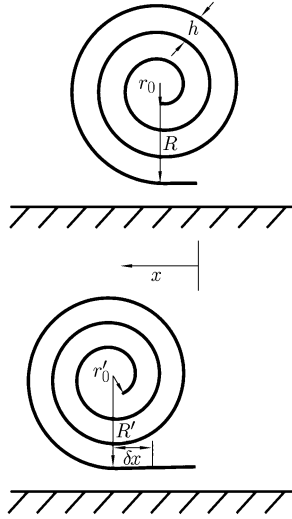


Fig. 8. Schematic illustration of CNS on substrate. As the CNS rolls forward with an infinitesimal displacement δx , the inner and outer radii of CNS change to r'_0 and R' from r_0 and R , respectively^[17].

The energy release rate per unit area, corresponding to the energetic force associated with unrolling, is therefore

$$\frac{f}{L} = -\frac{1}{L} \frac{\delta V}{\delta x} = \gamma_{CS} - \gamma_{CC} + \frac{D}{2[(B-x)h/\pi + r_0^2]} \quad (19)$$

The above equation shows that the net driving force can be either positive or negative, depending on the relative magnitudes of the self-affinity (γ_{CC}) of the graphene sheet and its affinity with the substrate (γ_{CS}). Assuming the system is mainly dominated by surface energy, the CNS would roll forward if $\gamma_{CS} - \gamma_{CC} > 0$, and backward if $\gamma_{CS} - \gamma_{CC} < 0$. Therefore, the translational motions of CNS can be fully controlled by adjusting the value of $\gamma_{CS} - \gamma_{CC}$. The equation of motion for such translational motion can be derived from Lagrange's equation

$$\frac{\partial (K - V)}{\partial x} - \frac{d}{dt} \left[\frac{\partial (K - V)}{\partial \dot{x}} \right] = 0 \quad (20)$$

(as before K denotes the kinetic energy and V the potential energy of the system; t is the time and over-dot the time derivative). To evaluate the kinetic energy of the system, we consider a rolling CNS as a rolling cylinder on a substrate with kinetic energy

$$K = \frac{1}{2} M \dot{x}^2 + \frac{1}{2} J_A \omega_A^2 \quad (21)$$

where $J_A = MR^2/2$ is the moment of inertia of the cylinder, $\omega_A = \dot{x}/R$ is the angular velocity and $M = \rho L(B-x) + M_0$ is the mass of the rolling CNS, ρ being the mass density of graphene and M_0 the mass of the constricting tube in the core. Inserting Eq.(21) into Eq.(20) yields

$$\frac{3}{2} [\rho L(B-x) + M_0] \ddot{x} - \frac{3}{4} \rho L \dot{x}^2 + L \left\{ \gamma_{CC} - \gamma_{CS} - \frac{D}{2[(B-x)h/\pi + r_0^2]} \right\} = 0 \quad (22)$$

Given initial conditions and properties of the CNS and substrate, Eq.(22) can be integrated to predict the translational motion of the CNS.

To verify the theoretical model, MD simulations are conducted with the non-bonded vdW interactions as described by the L-J potential as shown in Eq.(13) with the tuning parameter ($0 < \lambda \leq 1$) used to tune the strengths of CNS-CNS, CNS-CNT or CNS-substrate interactions. For all simulations, the CNS-graphite and CNS-CNT interactions are fixed by setting the tuning parameter at 0.8 and 1.0, respectively. The CNS-CNS interactions, however, are tuned to different levels by setting the tuning parameter at $\lambda_{CC} = 0.5, 0.6, 0.7$ to unroll the CNS leftward, or $\lambda_{CC} = 0.9, 1.0$ to roll it rightward.

Two layers of graphene with dimension $31 \times 3.8 \text{ nm}^2$ are used in the system: the bottom layer is fixed to model the graphite substrate and the top one is rolled up into a CNS with right end fixed. A MWCNT consisting of (5,5) and (10,10) SWCNTs is inserted into the core of CNS. Two initial configurations of partially rolled up CNSs are selected in the simulation: one with $x = 15.2 \text{ nm}$ (Fig.7(a)) and another with $x = 1.1 \text{ nm}$ (Fig.7(b)). The initial velocities are set to be zero.

To investigate the linear motion of CNS on substrate, Eq.(22) is numerically solved with additional parameters set as $\rho = 12 \times 1.66054 \times 10^{-27} / (3\sqrt{3}/4 \times 0.142^2 \times 10^{-18}) \text{ kg/m}^2$, $M_0 = 960 \times 12 \times 1.66054 \times 10^{-27} \text{ kg}$ and $L = 3.8 \text{ nm}$. The predicted motion of CNS for different tuning parameters, as shown in Figs.9(a) and 9(b) (dashed lines), agrees well with the corresponding MD results (scatters), indicating that the theoretical model is capable of predicting the rolling motion of CNS on substrate.

Constraining the core size of the CNS is essential in realizing the controlled translational motion of CNS on substrate. To demonstrate this, MD simulation is repeated without any insertion into CNS. The results are shown in Fig.10. It is seen that the CNS does not unroll leftward as the CNS-CNS interaction decreases. Instead it remains at the initial position while expanding its core (Fig.10, $t = 30 \text{ ps}$). This simulation shows that, when its core is unconstrained, frictionless layer sliding with core expansion is the preferred mode of energy reduction.

To reveal the underlying mechanism, the energy release rates associated with the rolling and expansion of CNS are compared. The energy release rate for expansion of CNS is obtained as

$$f_{\text{expansion}} = \frac{\pi D}{h} \frac{R^2 - r_0^2}{R^2} \frac{1}{r_0} - 2\pi\gamma_{CC} \left(1 + \frac{r_0}{R}\right) \quad (23)$$

and that for the rolling of CNS is given by Eq.(19). These energy release rates are plotted as a function of the core radius in Fig.11(a) with typical parameters for the CNS on graphite. Figure 11(b) plots the core radius as a function of surface energy of CNS. As an external field is applied, the surface

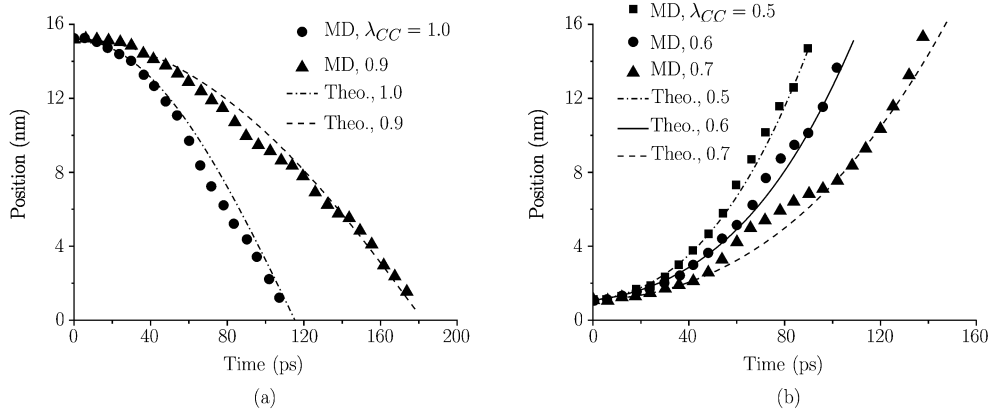


Fig. 9. Position of CNS as a function of time. Dash lines show the theoretical results and scatters show the MD results. The CNS rolls (a) rightward or (b) leftward with different CNS-CNS interactions^[17].

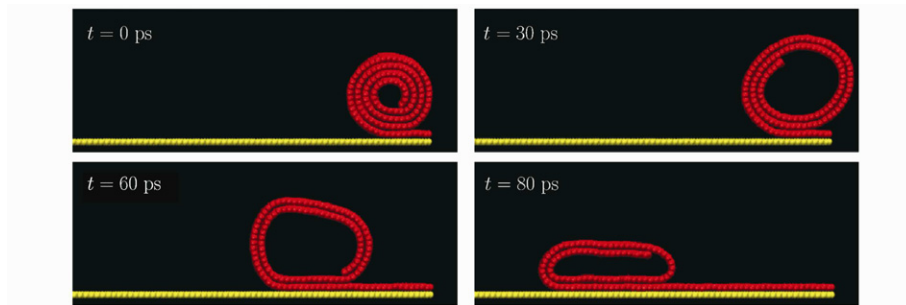


Fig. 10. Snapshots of MD simulation of CNS (red colour) expanding and rolling on the graphite substrate (yellow colour). The tuning parameters for CNS-CNS and CNS-graphite interactions are $\lambda_{CC} = 0.6$ and $\lambda_{CS} = 0.8$, respectively^[17].

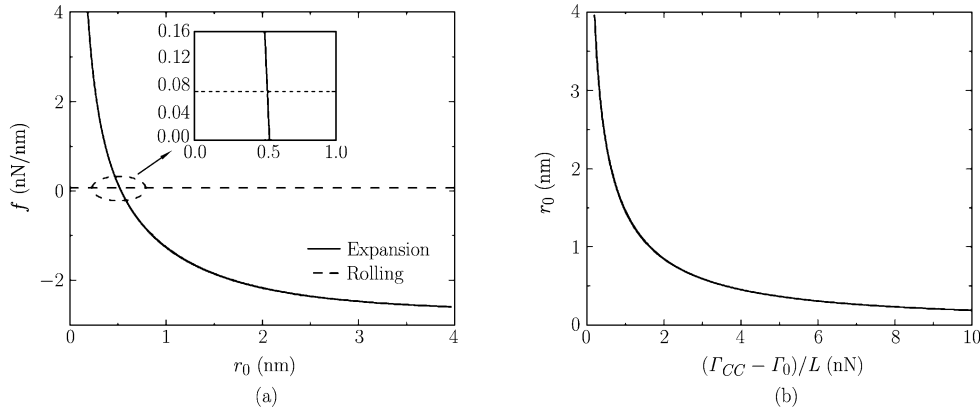


Fig. 11. Competing core expansion and rolling motion of a CNS on substrate. (a) The energy release rate associated with core expansion of a CNS is seen to easily dominate over that associated with the CNS rolling on a substrate as the system is perturbed away far from equilibrium by an external field, (b) the equilibrium core size as a function of the surface energy of CNS. The parameters are selected as $B = 31$ nm, $h = 0.34$ nm, $D = 0.11$ nNnm, $\lambda_{CC} = 0.6$ and $\lambda_{CS} = 0.8$ ^[17].

energy decreases while the equilibrium core radius increases. In this case, Fig.11(a) shows that there is a tendency for the CNS core to expand toward the new equilibrium size, with energy release rate orders of magnitude higher than that associated with the rolling motion.

Therefore, when an external field is applied to perturb the equilibrium state of CNS, the dominant mode of response of CNS is core expansion. As the inner core r_0 increases, the energy release rate $f_{\text{expansion}}$ associated with core expansion drops rapidly, and eventually the rolling motion is initiated for further energy reduction. As shown in Fig.10, the rolling motion starts only after substantial expansion of the inner core ($t = 60$ ps), at which the shape of CNS has changed so much that Eq. (4) can no longer be used to describe the elastic energy in the system. As the number of layers is reduced by core expansion, the CNS collapses on the substrate at $t = 80$ ps. In this situation, the motion of CNS is rather complicated and unpredictable. Thus the core size of CNS must be fully constrained in order to design a controllable CNS-based nanoactuator.

To further investigate the role of CNT insertion, Zhang and Li^[19] have studied this rolling problem through MD simulations and demonstrate that the CNT can also induce spontaneous rolling of a graphene sheet on substrate into CNS. The rolling process is controlled by the CNT size, the interlayer interaction energy of CNS, γ_{CC} , and the interaction energy per unit area between the rolled out graphene sheet and substrate, γ_{CS} . It is shown that CNT helps to overcome the energy barrier to form an overlap in graphene, which then spontaneously roll up into a CNS. The critical parameters governing the formation of CNS are elucidated through a phase diagram^[19]. Other studies on the formation of CNSs from graphene have also been investigated via MD simulations, e.g. nanodroplets assisting rolling of graphene^[23] and spontaneous rolling of graphene nanoribbons^[24, 25].

V. TUNABLE CORE SIZE OF CNS

As stated, the equilibrium core size of CNS is controlled by the surface energy of CNS, the bending modulus of graphene, the interlayer space and the basal graphene length. Changing any of these parameters would lead to variations, or tuning, of the core size of CNS. In particular, tuning the surface energy of CNS to control its core size seems feasible. Theoretically it has been demonstrated that the surface energy of CNS would decrease upon the application of an electric field^[18]. Thus the core size of CNS can be tuned through an electric field.

An applied electric field will cause carbon atoms to be polarized with the following dipole-dipole interactions^[26]

$$V(\mathbf{r}_{12}) = \frac{1}{4\pi\epsilon_0 |\mathbf{r}_{12}|^3} \left[|\mathbf{p}_1| |\mathbf{p}_2| - \frac{3(\mathbf{r}_{12} \cdot \mathbf{p}_1)(\mathbf{r}_{12} \cdot \mathbf{p}_2)}{|\mathbf{r}_{12}|^2} \right] \quad (24)$$

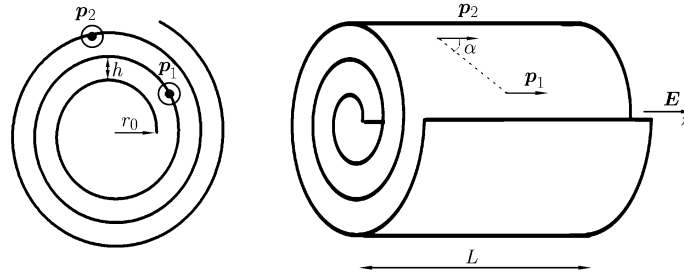


Fig. 12. Schematic illustration of two dipoles in CNS induced by an electric field applied in the axial direction^[18].

where $|\mathbf{r}_{12}|$ is the distance between dipole 1 and dipole 2, $\mathbf{p}_1 = 4\pi\epsilon_0\alpha_1\mathbf{E}$ is the induced dipole moment, \mathbf{E} being the applied electric field, ϵ_0 the vacuum permittivity and α_1 the polarizability of atom 1. It has been previously shown that the polarizability of single-walled carbon nanotubes (SWCNTs) in the axial direction is one order of magnitude higher than that perpendicular to the axis^[27]. Therefore, for simplicity, only the axial polarizability of carbon atoms in the CNS is considered. Consider two dipoles induced by electric field \mathbf{E} with dipole moment \mathbf{p}_1 and \mathbf{p}_2 as shown in Fig.12.

The distance of the two dipoles is

$$|\mathbf{r}_{12}| = \sqrt{\tilde{r}_1^2 + \tilde{r}_2^2 - 2\tilde{r}_1\tilde{r}_2 \cos(\theta_1 - \theta_2) + z^2} \quad (25)$$

where

$$\tilde{r}_1 = r_0 + \frac{h}{2\pi}\theta_1, \quad \tilde{r}_2 = r_0 + \frac{h}{2\pi}\theta_2 \quad (26)$$

Suppose each carbon atoms in the CNS is polarized in the electric field. The total dipole-dipole interaction is

$$\Phi_{\text{dipole}} = \sum_{i \neq j} V(\mathbf{r}_{ij}) \quad (27)$$

which can be calculated as

$$\begin{aligned} \Phi_{\text{dipole}} &= \rho_1\rho_2 \int_0^L dz' \int_0^{2\pi N} \tilde{r}_1 d\theta_1 \int_{\theta_1}^{2\pi N} \tilde{r}_2 d\theta_2 \\ &\cdot \int_{-z'}^{L-z'} \frac{1}{4\pi\epsilon_0 |\mathbf{r}_{12}^3|} (p_1 p_2 - 3p_1 p_2 \cos^2 \alpha) dz \end{aligned} \quad (28)$$

where ρ_1, ρ_2 are the dipole densities, N is the winding number of the CNS, $\cos \alpha = z/|\mathbf{r}_{12}|$. Integrating Eq.(28), one obtains

$$\Phi_{\text{dipole}} = \frac{(4\pi\epsilon_0 E)^2}{2\pi\epsilon_0} \rho_1\rho_2 e_{\text{dipole}}(N, L, r_0, t) \quad (29)$$

where

$$\begin{aligned} e_{\text{dipole}}(N, L, r_0, t) &= \int_0^{2\pi N} \int_{\theta_1}^{2\pi N} \tilde{r}_1 \tilde{r}_2 \alpha_1 \alpha_2 \left[\frac{1}{\sqrt{\tilde{r}_1^2 + \tilde{r}_2^2 - 2\tilde{r}_1 \tilde{r}_2 \cos(\theta_1 - \theta_2)}} \right. \\ &\quad \left. - \frac{1}{\sqrt{\tilde{r}_1^2 + \tilde{r}_2^2 + L^2 - 2\tilde{r}_1 \tilde{r}_2 \cos(\theta_1 - \theta_2)}} \right] d\theta_2 d\theta_1 \end{aligned} \quad (30)$$

The surface energy of the CNS due to dipole-dipole interaction can be extracted as

$$\gamma_{\text{dipole}} = \frac{1}{2\pi L} \frac{d\Phi_{\text{dipole}}}{d(r_0 + R)} \quad (31)$$

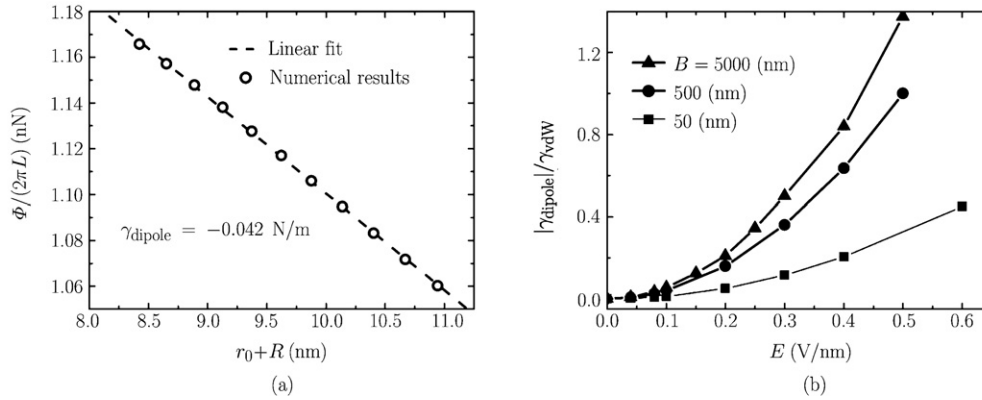


Fig. 13. (a) Dipole-dipole interaction energy of a CNS as a function of the sum of the inner and outer radii. The slope provides an estimate of the dipole induced surface energy of the CNS to be about -0.042 nN/nm with an electric field of $E=0.1$ V/nm, (b) dipole induced surface energy (normalized by vdW interaction energy) as a function of the applied electric field for different lengths of graphene^[18].

The total effective surface energy of the CNS is thus

$$\gamma_{\text{eff}} = \gamma_{\text{vdW}} + \gamma_{\text{dipole}} \quad (32)$$

where γ_{vdW} is the surface energy due to van der Waals interaction between carbon atoms. Figure 13(a) shows that the total dipole interaction energy is indeed linearly proportional to the sum of the inner and outer radii of the CNS, with a negative slope proportional to γ_{dipole} , in consistency with Eq.(31). The fact that γ_{dipole} is negative indicates that the applied electric field tends to decrease the effective surface energy. Figure 13(b) shows how the applied electric field influences the dipole induced surface energy γ_{dipole} normalized by γ_{vdW} , typically about 0.2 N/m. As the electric field \mathbf{E} varies in the range from 0 to 0.5 V/nm, the normalized dipole surface energy changes from 0 to 32.7% for $B = 50$ nm or from 0 to 100% for $B = 500$ nm, indicating that the electric field can significantly alter the surface energy^[28].

Based on such analysis, a class of novel, tunable water channels based on CNS was proposed with core radius tuned over a broad size range by an applied DC/AC electric field^[18]. The results demonstrated that it is possible to use dipole-dipole interaction induced by an externally applied electric field to reduce the effective surface energy of a CNS, so as to controllably increase its core size and the associated water flow rate. Compared with CNT-based water channels^[29–39], the CNS-based channels exhibit much greater water permeability and sensitivity to an applied DC/AC electric field. Beside applications as water channels, the tunable CNS channel model can also serve as ion channels across cellular membrane or controllable nanofilters to prevent the passing of heavy metal ions or nanoparticles.

VI. CONCLUSION

In this article, we have reviewed some of the recent theoretical and molecular dynamics investigations on the mechanics of carbon nanoscrolls, focusing on the structural and dynamical behaviors of these carbon-based materials. It has been shown theoretically that the core radius of a CNS depends on the surface energy, the bending stiffness, the interlayer spacing, the length of the basal graphene sheet, as well as the difference between the inner and outer pressures of CNS. A theoretical model to describe the ‘breathing’ oscillatory motion of CNS has also been reviewed. It has been shown that the gigahertz oscillation of CNS can be controlled by tuning the effective surface energy of the system via an applied DC/AC electric field. The results suggest possible applications of CNS as nanooscillators and nanoactuators. The resonant oscillation of a CNS near its fundamental frequency might be useful for molecular loading/release in gene and drug delivery systems. We have also reviewed a theoretical model based on the classical Lagrangian dynamics to describe the rolling and unrolling motions of CNS on substrate. It has been found that the theoretical model is fully capable of predicting molecular dynamics simulation results. It has been suggested that CNS based linear nanoactuators can be controlled by tuning the effective surface energy of the system via an applied DC/AC electric field as well as adjusting

the width of CNS. These results suggest promising applications of CNS as linear actuators and motors in nanomechanical systems. It has also been shown that an applied DC/AC field can effectively reduce the surface energy of CNS, so as to decrease the core size of CNS. These results suggest CNS can serve as controllable water/ion channels in biological systems.

References

- [1] Viculis,L.M., Mack,J.J. and Kaner,R.B., A chemical route to carbon nanoscrolls. *Science*, 2003, 299: 1361.
- [2] Xie,X., Ju,L., Feng,X.F., Sun,Y.H., Zhou,R.F., Liu,K., Fan,S.S., Li,Q.L. and Jiang,K.L., Controlled fabrication of high-quality carbon nanoscrolls from monolayer graphene. *Nano Letters*, 2009, 9: 2565-2570.
- [3] Savoskin,M.V., Mochalin,V.N., Yaroshenko,A.P., Lazareva,N.I., Konstantinova,T.E., Barsukov,I.V. and Prokofiev,L.G., Carbon nanoscrolls produced from acceptor-type graphite intercalation compounds. *Carbon*, 2007, 45: 2797-2800.
- [4] Roy,D., Angeles-Tactay,E., Brown,R.J.C., Spencer,S.J., Fry,T., Dunton,T.A., Young,T. and Milton,M.J.T., Synthesis and raman spectroscopic characterisation of carbon nanoscrolls. *Chemical Physics Letters*, 2008, 465: 254-257.
- [5] Chuvilin,A.L., Kuznetsov,V.L. and Obraztsov,A.N., Chiral carbon nanoscrolls with a polygonal cross-section. *Carbon*, 2009, 47: 3099-3105.
- [6] Shioyama,H. and Akita,T., A new route to carbon nanotubes. *Carbon*, 2003, 41: 179-181.
- [7] Chen,Y., Lu,J. and Gao,Z.X., Structural and electronic study of nanoscrolls rolled up by a single graphene sheet. *The Journal of Physical Chemistry C*, 2007, 111: 1625-1630.
- [8] Braga,S.F., Coluci,V.R., Legoas,S.B., Giro,R., Galvao,D.S. and Baughman,R.H., Structure and dynamics of carbon nanoscrolls. *Nano Letters*, 2004, 4: 881-884.
- [9] Braga,S.F., Coluci,V.R., Baughman,R.H. and Galvao,D.S., Hydrogen storage in carbon nanoscrolls: an atomistic molecular dynamics study. *Chemical Physics Letters*, 2007, 441: 78-82.
- [10] Coluci,V.R., Braga,S.F., Baughman,R.H. and Galvao,D.S., Prediction of the hydrogen storage capacity of carbon nanoscrolls. *Physical Review B*, 2007, 75: 125404.
- [11] Mpourmpakis,G., Tyliaakis,E. and Froudakis,G.E., Carbon nanoscrolls: a promising material for hydrogen storage. *Nano Letters* 2007, 7: 1893-1897.
- [12] Pan,H., Feng,Y. and Lin,J., An initio study of electronic and optical properties of multiwall carbon nanotube structures made up of a single rolled-up graphite sheet. *Physical Review B*, 2005, 72: 085415.
- [13] Rurali,R., Coluci,V.R. and Galvao,D.S., Prediction of giant electroactuation for papyruslike carbon nanoscroll structures: first-principles calculations. *Physical Review B*, 2006, 74: 085414.
- [14] Shi,X.H., Pugno,N.M. and Gao,H.J., Tunable core size of carbon nanoscrolls. *Journal of Computational and Theoretical Nanoscience*, 2010, 7: 517-521.
- [15] Shi,X.H., Pugno,N.M. and Gao,H.J., Constitutive behavior of pressurized carbon nanoscrolls. *International Journal of Fracture*, 2010, Doi: 10.1007/s10704-010-9545-y.
- [16] Shi,X.H., Cheng,Y., Pugno,N.M. and Gao,H.J., Gigahertz breathing oscillators based on carbon nanoscrolls. *Applied Physics Letters*, 2009, 95: 163113.
- [17] Shi,X.H., Cheng,Y., Pugno,N.M. and Gao,H.J., A translational nanoactuator based on carbon nanoscrolls on substrates. *Applied Physics Letters*, 2010, 96: 053115.
- [18] Shi,X.H., Cheng,Y., Pugno,N.M. and Gao,H.J., Tunable water channels with carbon nanoscrolls. *Small*, 2010, 6: 739-744.
- [19] Zhang,Z. and Li,T., Carbon nanotube initiated formation of carbon nanoscrolls. *Applied Physics Letters*, 2010, 97: 081909.
- [20] Hess,B., Kutzner,C., van der Spoel,D. and Lindahl,E., Gromacs 4: algorithms for highly efficient, load-balanced, and scalable molecular simulation. *Journal of Chemical Theory and Computation*, 2008, 4: 435-447.
- [21] Walther,J.H., Jaffe,R., Halicioglu,T. and Koumoutsakos,P., Carbon nanotubes in water: structural characteristics and energetics. *Journal of Physical Chemistry B*, 2001, 105: 9980-9987.
- [22] Plimpton,S., Fast parallel algorithms for short-range molecular-dynamics. *Journal of Computational Physics*, 1995, 117: 1-19.
- [23] Patra,N., Wang,B.Y. and Král,P., Nanodroplet activated and guided folding of graphene nanostructures. *Nano Letters*, 2009, 9: 3766-3771.
- [24] Martins,B.V.C. and Galvao,D.S., Curved graphene nanoribbons: structure and dynamics of carbon nanobelts. *Nanotechnology*, 2010, 21: 075710.
- [25] Xu,Z.P. and Buehler,M.J., Geometry controls conformation of graphene sheets: membranes, ribbons, and scrolls. *ACS Nano*, 2010, 4: 3869-3876.
- [26] Israelachvili,J., Intermolecular & Surface Forces. London: Academic Press, 1991.

- [27] Langlet,R., Devel,M. and Lambin,P., Computation of the static polarizabilities of multi-wall carbon nanotubes and fullerites using a gaussian regularized point dipole interaction model. *Carbon*, 2006, 44: 2883-2895.
- [28] Fogler,M.M., Castro Neto,A.H. and Guinea,F., Effect of external conditions on the structure of scrolled graphene edges. *Physical Review B*, 2010, 81: 161408.
- [29] Hummer,G., Rasaiah,J.C. and Noworyta,J.P., Water conduction through the hydrophobic channel of a carbon nanotube. *Nature*, 2001, 414: 156-159.
- [30] Garate,J.A., English,N.J. and MacElroy,J.M.D., Carbon nanotube assisted water self-diffusion across lipid membranes in the absence and presence of electric fields. *Molular Simulation*, 2009, 35: 3-12.
- [31] Zhu,F.Q. and Schulten,K., Water and proton conduction through carbon nanotubes as models for biological channels. *Biophysical Journal*, 2003, 85: 236-244.
- [32] Wan,R.Z., Li,J.Y., Lu,H.J. and Fang,H.P., Controllable water channel gating of nanometer dimensions. *Journal of the American Chemical Society*, 2005, 127: 7166-7170.
- [33] Joseph,S. and Aluru,N.R., Pumping of confined water in carbon nanotubes by rotation-translation coupling. *Physical Review Letters*, 2008, 101: 064502.
- [34] Liu,B., Li,X.Y., Li,B.L., Xu,B.Q. and Zhao,Y.L., Carbon nanotube based artificial water channel protein: Membrane perturbation and water transportation. *Nano Letters*, 2009, 9: 1386-1394.
- [35] Zou,J., Ji,B.H., Feng,X.Q. and Gao,H.J., Molecular-dynamic studies of carbon-water-carbon composite nanotubes. *Small*, 2006, 2: 1348-1355.
- [36] Yuan,Q.Z. and Zhao,Y.P., Hydroelectric voltage generation based on water-filled single-walled carbon nanotubes. *Journal of the American Chemical Society*, 2009, 131: 6374-6376.
- [37] Mashl,R.J., Joseph,S., Aluru,N.R. and Jakobsson,E., Anomalously immobilized water: A new water phase induced by confinement in nanotubes. *Nano Letters*, 2003, 3: 589-592.
- [38] Gong,X.J., Li,J.Y., Lu,H.J., Wan,R.Z., Li,J.C., Hu,J. and Fang,H.P., A charge-driven molecular water pump. *Nature Nanotechnology*, 2007, 2: 709-712.
- [39] Li,J.Y., Gong,X.J., Lu,H.J., Li,D., Fang,H.P. and Zhou,R.H., Electrostatic gating of a nanometer water channel. *Proceedings of the National Academy of Sciences of the United States of America*, 2007, 104: 3687-3692.